Polymer 51 (2010) 3099–3107

Contents lists available at ScienceDirect

Polymer

journal homepage: www.elsevier.com/locate/polymer

Benzo[1,2-b:4,5-b′]dithiophene-based copolymers applied in bottom-contact field-effect transistors

Mark A.M. Leenen [a,b], Fabio Cucinotta [b], Wojciech Pisula [c,d], Jürgen Steiger [a], Ralf Anselmann [a], Heiko Thiem [a,*], Luisa De Cola [b]

[a] Evonik Degussa GmbH, Creavis – Technologies and Innovation, Paul-Baumann-Straße 1, D-45764 Marl, Germany
[b] Physikalisches Institut and Center for Nanotechnology, CeNTech, Universität Münster, Mendelstraße 7, D-48149 Münster, Germany
[c] Max Planck Institute for Polymer Research, Ackermannweg 10, D-55128 Mainz, Germany
[d] Evonik Degussa GmbH, Process Technology & Engineering, Process Technology – New Processes, Rodenbacher Chaussee 4, D-63457 Hanau-Wolfgang, Germany

ARTICLE INFO

Article history:
Received 19 January 2010
Received in revised form
3 May 2010
Accepted 13 May 2010
Available online 25 May 2010

Keywords:
Polymer synthesis
Polymer materials

ABSTRACT

Three copolymers of benzo[1,2-b:4,5-b′]dithiophene and 3,3′-bis(alkyl)-5,5′-bithiophene (dodecyl, tetradecyl and hexadecyl side chains) have been synthesized through Stille copolymerization. The polymers have number-average molecular weights over 20 kg/mol, are well-packed in the bulk and thin film, and possess an ionization potential of −5.1 eV in thin film, which offers stability versus oxidation in environmental conditions. The thin film packing of the polymer with dodecyl side chains leads to an excimeric emission upon excitation, which is not observed for longer side chain lengths. The presence of the dimers responsible for this excimer formation results in a device performance improvement as well. Field-effect transistors fabricated from these copolymers have On/Off ratios $>10^7$, equal saturation and linear hole mobilities above 10^{-2} cm^2/Vs, almost no hysteresis and turn-on voltages around 0 V in bottom-contact devices.

1. Introduction

In the past decade, research towards solution-processed organic semiconductors has increased tremendously [1,2], because these materials are envisioned to enable low-cost electronics on flexible surfaces [3]. Although the film-forming properties of (amorphous or semicrystalline) conjugated polymers are superior to those of small (crystalline) molecules, the material performance (charge carrier mobility) is generally in favor of small molecules [4–6]. Nevertheless, also polymers are currently able to obtain mobilities in excess of 0.5 cm^2/Vs [7–10], the benchmark performance of amorphous silicon.

A commonly used building block, for p-type semiconducting polymers, is benzo[1,2-b:4,5-b′]dithiophene (BDT). The 4,8-substitution with alkyl side chains, has already resulted in materials employed in organic field-effect transistors (OFETs) with hole mobilities exceeding 0.1 cm^2/Vs [11,12]. Also poly[2,6-bis(3-dodecylthiophen-2-yl) benzo[1,2-b:4,5-b′]dithiophene] (PTBT), a polymer of BDT substituted with 3-alkylthiophenes, has been reported [13,14]. The low reported mobility of PTBT (8×10^{-5} cm^2/Vs), synthesized by oxidative polymerization [13], prompted us to resynthesize it by Stille copolymerization. The resynthesized copolymer **1a** (Scheme 1) showed a hole mobility of 10^{-2} cm^2/Vs in bottom-contact geometry, a performance improvement of over a factor 100 (vide infra). During these measurements, a different research group has reported polymer **1a** in a top-contact device geometry as well [14].

In this work, we have synthesized two additional polymers with longer alkyl side chain lengths, in order to understand the role played by the side chain length elongation on the material performance. In fact it was shown for different types of systems that such an increased side chain length can result in an improved performance [8,15]. Thus, we have synthesized two new poly[2,6-bis(3-alkylthiophen-2-yl)benzo[1,2-b:4,5-b′]dithiophene]s, with tetradecyl **1b** and hexadecyl **1c** side chains (Scheme 1). Furthermore, by utilizing a Soxhlet extraction, we have greatly improved the molecular weight, the On/Off ratio and hysteresis of **1a** [14]. Finally, we have optimized the OFET performance of these copolymers in bottom-contact (BC) device geometry. Although a top-contact (TC) device geometry generally gives higher mobility values, material parameters can be more reliably evaluated in the BC geometry [16] and additionally, the BC geometry is most relevant for industrial application of OFETs.

* Corresponding author. Tel.: +49 2365 49 9483; fax: +49 2365 49 80 9483.
E-mail address: heiko.thiem@evonik.com (H. Thiem).

0032-3861/$ – see front matter © 2010 Elsevier Ltd. All rights reserved.
doi:10.1016/j.polymer.2010.05.022

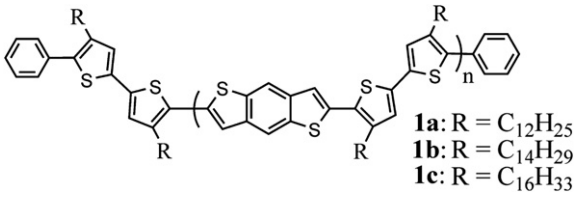

Scheme 1. Synthesized copolymers in this work.

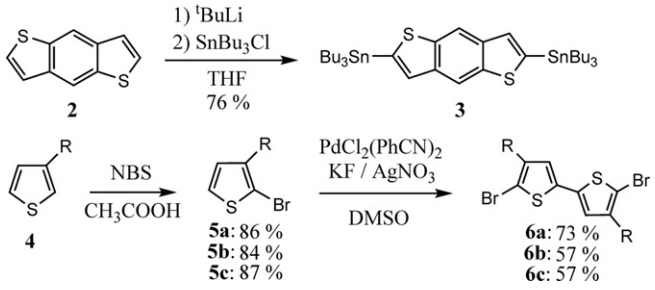

Scheme 2. Synthesis of Monomer 1 and Monomer 2. **4a**, **5a**, **6a**: R = $C_{12}H_{25}$. **4b**, **5b**, **6b**: R = $C_{14}H_{29}$. **4c**, **5c**, **6c**: R = $C_{16}H_{33}$.

2. Synthesis

The synthesis of both monomers is depicted in Scheme 2. BDT **2** has been synthesized according to modified literature procedures [17]. 2,6-Bis(tributylstannyl)benzo[1,2-b:4,5-b′]dithiophene **3** (Monomer 1) has been synthesized from **2** by direct lithiation of the 2- and 6-positions, followed by the addition of tributylstannyl-chloride. The colorless oil was obtained in good yields.

2-Bromo-3-alkylthiophenes **5a**–**5c** were synthesized by selective bromination of corresponding 3-alkylthiophenes **4a**–**4c** with NBS in glacial acetic acid in high yields. 2,2′-Dibromo-3,3′-bis (alkyl)-5,5′-bithiophenes **6a**–**6c** (Monomer 2) were obtained by homocoupling of 2-bromo-3-alkylthiophenes **5a**–**5c** at the 5-position of the molecule. This extraordinary homocoupling, where the bromide functional group is preserved, was undertaken in warm DMSO, with $PdCl_2(PhCN)_2$ as catalyst, in the presence of $AgNO_3$ and KF [18,19].

The copolymers **1a**–**1c** were obtained through Stille copolymerization (Scheme 3) in good yields, determined from the combined chloroform, chlorobenzene (CB) and 1,2-dichlorobenzene (ODCB) fractions after Soxhlet extraction. A rather large excess of Monomer 2 (1.04 eq with respect to Monomer 1) has been used to tune chain length and therewith solubility, processability and polymerization yield. Additionally, almost each polymer chain should have the bithiophene monomeric unit at both chain ends by using such an excess.

To remove bromo- and tributyltin end-groups, the polymers have been end-capped with phenyl-groups, by subsequent addition of tributylphenyltin and bromobenzene after the polymerization was completed. Without defined end-capping, remaining end-groups can act as charge carrier trap sites [20,21], or can disturb local film morphology [22]. Both effects are detrimental to device performance.

3. Polymer characterization

The molecular weights of the synthesized copolymers, determined by gel permeation chromatography (GPC), are summarized in Table 1. In all CB fractions, the number-average molecular weight, M_n, is over 20 kg/mol, with a maximum M_n of 43 kg/mol for **1a**. Responsible for the higher average molecular weights, compared to the polymer reported in recent literature (M_n 17 kg/mol, M_w 42 kg/mol) [14], is the Soxhlet extraction that successfully extracts oligomers and short polymer chains first, before collecting the polymer fraction that will be used for device purposes.

The smallest polydispersity index (PDI) was found for **1a**, amounting to 1.8 for the CB fraction. Also the low PDI of the polymer batches, in this work, is a direct result of the Soxhlet extractions. The weight-average molecular weight, M_w, of each $CHCl_3$ fraction is smaller than the M_n of the corresponding CB fraction. Peak molecular weights, M_p, of **1a**–**1c** are comparable for both the $CHCl_3$ (12–13 kg/mol) and CB (35–41 kg/mol) fractions. Polymer degradation could be responsible for the lower M_n and M_w of the ODCB fraction of **1b**, compared to the CB fraction, due to the high ODCB reflux temperatures during the Soxhlet extraction procedure.

The polymers were characterized by ^{1}H NMR (solutions of the $CHCl_3$ fractions in deuterated 1,1,2,2-tetrachloroethane) and IR spectroscopy (CB fractions as powder); both are in agreement with data reported earlier on structurally similar polymers [12,13]. In the IR spectra, there is almost no distinction possible between **1a**–**1c**. The different alkyl chain lengths can however be detected in the ^{1}H NMR spectra by the magnitude of the integration of the signal around 1.00–1.50 ppm (see Experimental section). For all further characterization and device fabrication, the CB fractions of the polymers were used (unless stated differently).

We confirm the reported large tendency to aggregate of **1a** in diluted solution [14], which takes place to the same extent for **1b** and **1c**. Such aggregate formation has been reported before for similar copolymers as well [23]. Therefore, UV–Vis absorption spectra have been recorded in heated solutions (60 °C, chlorobenzene). As expected, the photophysical properties of copolymers **1a**–**1c** in heated solution are all comparable, with an optical band gap (E_g) of 2.12 eV. Representative UV–Vis absorption spectra of **1b** in solution, both heated and at room temperature, are shown in Fig. 1.

The UV–Vis absorption spectra of compounds **1a**–**1c**, recorded on drop-cast thin films, are shown in Fig. 2. For **1a**, **1b** and **1c**, the spectral pattern consists of a broad, slightly structured band centered around 515 nm with a shoulder at about 550 nm. The optical band gap E_g of **1a** is smaller than E_g of **1b** and **1c**, that have equal photophysical properties in thin film. For the $CHCl_3$ fraction of **1a**, the absorption peak is hypsochromically shifted to 473 nm, as expected because of the lower molecular weight of the polymer. As a consequence, the optical band gap for the $CHCl_3$ fraction of **1a** is estimated to be 2.18 eV, more than 0.1 eV larger than those obtained for the CB fractions of **1a**–**1c** (Table 2).

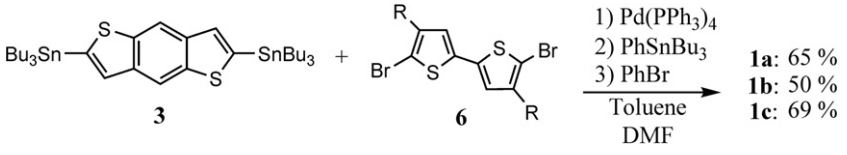

Scheme 3. Stille copolymerization.

Table 1
GPC data of synthesized copolymers versus polystyrene standards, determined with RI detector.

Polymer	Fraction	M_p (kg/mol)	M_n (kg/mol)	M_w (kg/mol)	PDI
1a	$CHCl_3$	13	11	17	1.6
1a	CB	38	43	76	1.8
1b	$CHCl_3$	13	12	19	1.5
1b	CB	35[a]	22[a]	69[a]	3.1[a]
1b	ODCB	52	20	66	3.3
1c	$CHCl_3$	12	9	15	1.8
1c	CB	41	29	116	4.0

[a] Determined with UV–Vis detector.

The emission spectra of **1a**–**1c** in heated chlorobenzene solutions are about equal and structured, with peaks at 540 nm and 585 nm (Fig. 3). It is noteworthy that neat films of **1a** (both the CB and the $CHCl_3$ fraction) display a larger red-shift and a de-structuring of emission (Fig. 3a and b) compared to the spectra of **1b** and **1c** (Fig. 3c and d), indicating a higher structural ordering. Based on this observation, we ascribe the different photophysical properties of **1a** not to the larger molecular weight of the CB fraction compared to **1b** and **1c**, but to the possible formation of an excimer due to the tilting of adjacent polymer chains, leading to an electronic interaction between neighbouring BDT cores. Apparently, the longer tetradecyl **1b** and hexadecyl **1c** side chains do not allow for the formation of such an excimer.

X-ray diffraction (XRD) measurements show an ordering of **1a**–**1c** in thin films (Fig. 4). The films were drop cast from 1,2-dichlorobenzene (ODCB) solutions on octyltrichlorosilane-pretreated silicon substrates. From 2-dimensional wide-angle X-ray scattering (2D-WAXS) experiments on extruded fibers of **1a** and **1b** (Fig. 5), a π–π inter-chain stacking distance of 0.37 nm (in accordance with literature [14]), and a chain-to-chain spacing related to side chain length (1.87 nm for **1a** and 2.1 nm for **1b**) can be extracted (Fig. 6). The latter values are in agreement with the XRD-measurements in thin film ($d = 1.87$ nm for **1a**, $d = 2.05$ nm for **1b**, $d = 2.18$ nm for **1c**), where the diffraction angle also clearly decreases with increasing side chain length (Fig. 4). Both in bulk fiber and in thin film, **1b** shows diffraction peaks with a higher intensity than **1a** and **1c**. This could be explained by the excimer formation in case of **1a**; even a small amount of inter-chain BDT-dimers, that result in excimeric emission upon excitation, could not only totally quench fluorescence, but would also disturb supramolecular ordering to the extent shown in Figs. 4 and 5. On the other hand, the hexadecyl side chains of **1c** seem to have crossed the upper limit for side chain length that still results in a strongly defined packing of the material.

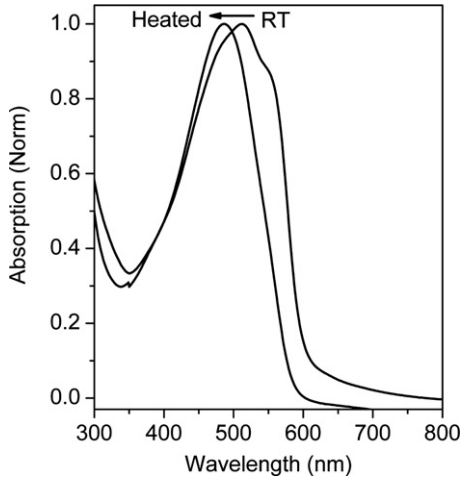

Fig. 1. Absorption spectra of the CB fraction of **1b**, in chlorobenzene solution at room temperature (RT) and heated to 60 °C.

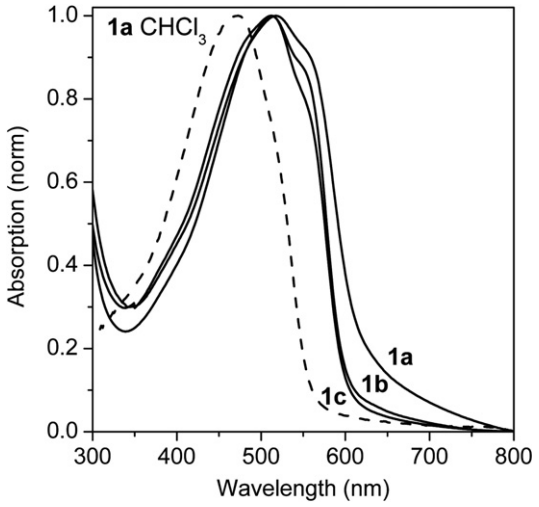

Fig. 2. Absorption spectra of **1a** ($CHCl_3$ fraction, dashed), and the CB fractions of **1a**, **1b** and **1c** (solid lines) in thin films.

Thermogravimetric analysis (TGA) shows a thermal stability of the copolymers up to over 400 °C in N_2-atmosphere. Subsequent differential scanning calorimetry (DSC) traces are featureless, and show no melting transitions or mesophases, comparable to a similar dithienothiophene-based copolymer [23] but contrary to PBTTT [8]. Also in temperature-dependent polarized optical microscopy experiments, no phase transitions have been observed.

Finally, the ionization potentials IP of the polymers in thin film were determined by UV Photoelectron Spectroscopy in air (PESA). The ionization potential did not show a dependence on side chain length, and was determined to be 5.1 ± 0.02 eV. This ionization potential is excellent for hole injection from clean gold contacts, and is indicative of stability versus oxidation in ambient conditions [24].

4. OFET characterization

Bottom gate, bottom-contact OFETs were fabricated to test the electrical characteristics of these copolymers. The surface of the

Table 2
Photophysical data of **1a**–**1c**.

Solution (60 °C)	**1a** ($CHCl_3$)	**1a** (CB)	**1b** (CB)	**1c** (CB)
λ_{abs} (nm)[a]	458	497	487	490
ε_{max} (M^{-1} cm^{-1})[a]	70,282	48,406	33,074	28,713
λ_{em} (nm)[a]	541	543	545	542
	580	583	579	580
ϕ_{em}[a]	3%	3%	3%	3%
E_g (eV)[a,b]	2.25	2.12	2.12	2.12
Neat films				
λ_{abs} (nm)[c]	473	518	512	513
λ_{em} (nm)[c]	670	670	562	561
			601	596
ϕ_{em}[c]	1%	1%	1%	1%
E_g (eV)[c,d]	2.18	2.01	2.06	2.06

[a] Values obtained from chlorobenzene solutions heated to 60 °C by a heating bath.
[b] Values obtained from the onset of the absorption spectra (551 nm for **1a** ($CHCl_3$), 585 nm for the CB fractions of **1a**–**1c**).
[c] Values obtained from drop cast films out of a 0.02 M $CHCl_3$ solution.
[d] Values obtained from the onset of the absorption spectra (570 nm for **1a** ($CHCl_3$), 618 nm for **1a**, 602 nm for **1b** and **1c**).

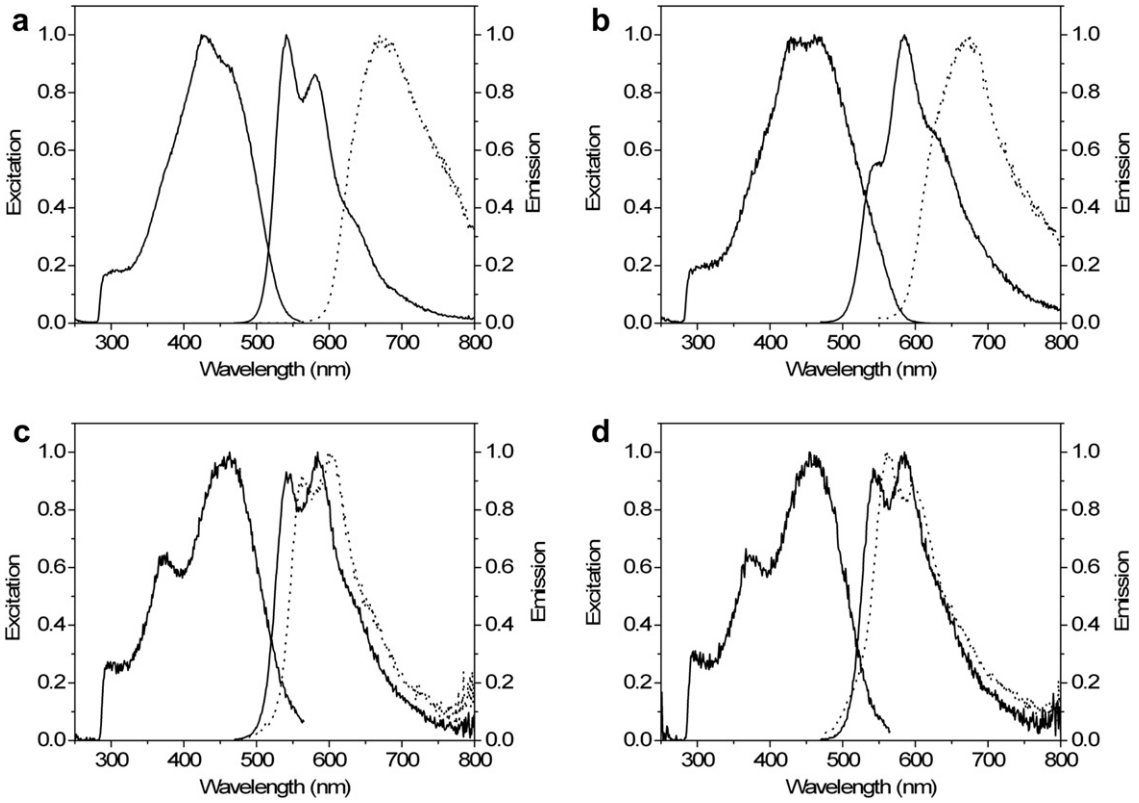

Fig. 3. (a) Normalized excitation (λ_{em} = 640 nm) and emission (λ_{exc} = 450 nm) spectra of **1a** ($CHCl_3$ fraction) in chlorobenzene solution (solid line) and emission spectrum of **1a** ($CHCl_3$ fraction) in thin film (dotted line). (b) Normalized excitation (λ_{em} = 640 nm) and emission (λ_{exc} = 450 nm) spectra of **1a** in chlorobenzene solution (solid line) and emission spectrum of **1a** in thin film (dotted line). The smaller intensity of the first emission band around 550 nm is due to self-absorption. (c) Normalized excitation (λ_{em} = 585 nm) and emission (λ_{exc} = 450 nm) spectra of **1b** in chlorobenzene solution (solid line) and emission spectrum of **1b** in thin film (dotted line). (d) Normalized excitation (λ_{em} = 585 nm) and emission (λ_{exc} = 450 nm) spectra of **1c** in chlorobenzene solution (solid line) and emission spectrum of **1c** in thin film (dotted line).

thermally grown SiO_2 dielectric was pretreated with trimethylchlorosilane (TMCS) or octyltrichlorosilane (OTS) to obtain a hydrophobic monolayer, on which the polymers could be spin-coated or drop cast from ODCB-solutions. After coating the semiconductor layer, the devices were annealed in a glovebox for 30 min at 130 °C to remove residual solvent and induce film ordering. OFET performance is summarized in Table 3.

From the transfer characteristics of **1a**–**1c**, drop cast from ODCB on TMCS (Fig. 7, left), it is clear that **1a** and **1b** perform considerably

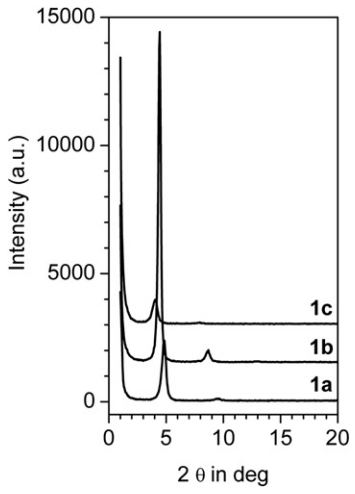

Fig. 4. XRD-spectra of **1a**–**1c** in drop cast thin films.

better than **1c**. This can be explained by the side chain length elongation in this series: the longer the side chain, the larger the influence of the insulating side chains will be on film formation and on the semiconductor film morphology at interfaces. Remarkably, **1a** performs slightly better than **1b**, although drop cast thin films of **1b** show stronger reflections in XRD than films of **1a**. Apparently, the tilted parts of the polymer chains of **1a** do not only allow for excimer formation, but they also facilitate charge transport along the channel, possibly by adding a third dimension for fast inter-chain charge transport. However, just like in case of **1b** and **1c**, the OFET performance (hole mobility) of the $CHCl_3$ fraction of **1a** is one order of magnitude lower than the mobility of the CB fraction, underlining the strong dominance of molecular weight on device performance.

Drop-casting results in rather rough and thick films ($d > 500$ nm), therefore spin-coating was preferentially used for further device optimization. Additionally, **1a** was coated on substrates with OTS monolayers. Organic thin films coated on OTS tend to be of high quality [12,25], leading to improved device performances compared to films coated on for instance TMCS. Next to that, spin-coating **1b** and **1c** on TMCS resulted in lower μ_h than for devices fabricated by drop-casting on TMCS (Table 3).

Transfer characteristics of **1a** spun on OTS are shown in Fig. 7 (right). Striking is the near-absence of hysteresis [26]. Secondly, the linear and the saturation mobility (μ_{lin} and μ_{sat}, respectively) are equal and amount to $1.4 \cdot 10^{-2}$ cm^2/Vs, whereas in most cases the linear mobility is usually a bit lower than the saturation mobility. Compared to the devices reported in literature [14], the On/Off ratio of OFETs of **1a** has been improved by over a factor 100,

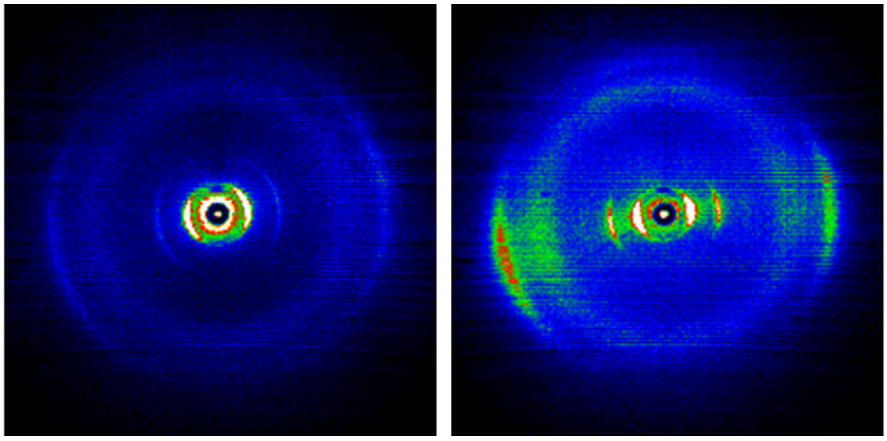

Fig. 5. 2D-WAXS patterns of **1a** (left) and **1b** (right) after annealing an extruded fiber at 180 °C.

and the hysteresis has been greatly decreased. Additionally, the same hole mobility has been achieved in a bottom-contact (BC) geometry as previously reported in a top-contact (TC) geometry [14]. Because TC OFETs have a better interface between the semiconductor layer and the contacts, compared to BC OFETs, they usually perform better than BC OFETs.

Responsible for the better performance of these batches of copolymers, compared to the polymer reported in literature [14], is likely the Soxhlet extraction. This extraction has resulted in a higher molecular weight and narrower PDI on the one hand, and possibly lower impurity concentrations (that could act as dopants [27]) on the other hand [28]. A small additional factor could be the polymer chain end-capping.

Ionization potentials determined by PESA indicated that **1a**–**1c** would be stable versus oxidation in environmental conditions. Therefore, OFETs of **1a** were also operated in air. Transfer characteristics of **1a** in air are shown in Fig. 8. Immediately clear is the increase in OFF current by a factor 100, and the appearance of hysteresis. Both effects are reversible: if the device, measured in air, is returned into a glovebox and shortly annealed, the original characteristics obtained in the glovebox are re-obtained. Measurements in air confirm that there is no irreversible oxidation of the polymers taking place in environmental conditions. On/Off ratios are still $>10^5$, and the charge carrier mobility is 8.5×10^{-3} cm^2/Vs, only slightly decreased compared to measurements in the glovebox. The turn-on voltage is unaffected. Ongoing dedicated long-term stability experiments suggest a strong dominance of physical, reversible effects over (electro) chemical, irreversible effects taking place.

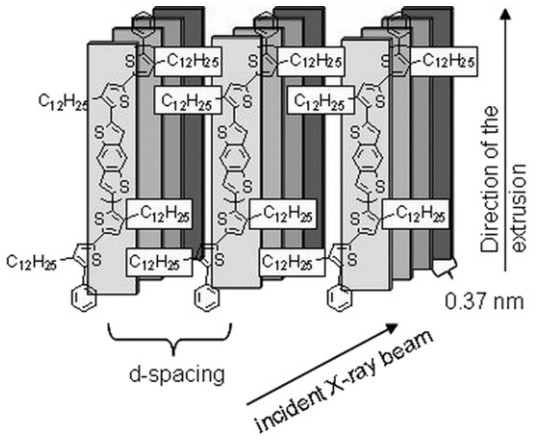

Fig. 6. Molecular ordering in an extruded fiber of **1a**, derived from 2D-WAXS experiments. The vertical lamellae correspond to the polymer long-axis along the conjugated backbone.

5. Conclusion

Three copolymers of BDT and bis(3-alkylthiophene)s have been synthesized by Stille coupling (dodecyl, tetradecyl and hexadecyl side chains) and subsequently purified and fractionated by Soxhlet extraction. The CB fractions of the polymers all had an $M_n > 20$ kg/mol. No liquid crystalline phases were observed in DSC traces. To prevent aggregation, UV–Vis absorption, excitation and photoluminescence spectra were recorded on heated solutions of the polymers. The emission spectrum of the dodecyl-substituted copolymer in thin film was distinctly different from the other two polymers, showing a red-shifted, 'excimer-like' unstructured emission, both for the $CHCl_3$ and the CB fractions. Our hypothesis for the occurrence of such an emission spectrum is the formation of excimers by tilted neighbouring polymer chains, resulting in an additional electronic interaction between BDT cores. The longer tetradecyl and hexadecyl side chains do not allow for the formation of such an excimer.

All polymers form ordered thin films, as studied by XRD. The ionization potentials, determined in thin film in air, amount to −5.1 eV, indicative of stability versus oxidation in environmental conditions. The best OFET performance in this series is obtained with the dodecyl side chains, resulting in hole mobilities amounting to 1.4×10^{-2} cm^2/Vs, On/Off ratios $>10^7$, a negligible hysteresis and turn-on voltages around 0 V in the industrially relevant bottom-contact geometry. In air, the OFF current and hysteresis are increased but no irreversible device degradation is taking place during operation.

The results obtained in this work suggest that a polymer fractionation and purification by Soxhlet extraction, which is being omitted regularly, can clearly improve material performance in thin film devices. We argue that the lower polymerization yield by fractionation, and Soxhlet processing time are fully compensated by better material performance. Furthermore, it is not unthinkable that the excimer formation observed for the polymers described in this work, can also occur for other fused conjugated cores with a suitable inter-chain spacing. The accompanying device performance improvement may suggest the incorporation of excimeric dimers as a new design tool for high-performance OFET materials.

Table 3
OFET performance of **1a**–**1c**.

Polymer, coating method	Silane, device geometry	μ_{sat} (cm^2/Vs)	μ_{lin} (cm^2/Vs)	On/off	$V_{turn\text{-}on}$ (V)	V_{th} (V)
1a, drop cast	Bare, BC	7.5×10^{-3}	3.5×10^{-3}	3×10^5	−14	−25
1a, drop cast	TMCS, BC	1.2×10^{-2}	10^{-2}	$>10^7$	0	−21
1b, drop cast	TMCS, BC	9×10^{-3}	7.5×10^{-3}	$>10^7$	−10	−27
1b, spun	TMCS, BC	6×10^{-3}	4×10^{-3}	$>10^7$	−4	−25
1c, drop cast	TMCS, BC	3×10^{-3}	1.2×10^{-3}	6×10^5	−6	−33
1c, spun	TMCS, BC	2×10^{-3}	1.5×10^{-3}	10^6	−12	−36
1a, drop cast	OTS, BC	10^{-2}	6.5×10^{-3}	$>10^7$	0	−21
1a, spun	OTS, BC	1.4×10^{-2}	1.4×10^{-2}	$>10^7$	0	−23
1a, spun, air	OTS, BC	8.5×10^{-3}	7×10^{-3}	2.5×10^5	0	−21
1a spun [14]	HMDS, TC	1.5×10^{-2}	–	10^{5}[a]	−4[a]	−20[a]
1a spun [13]	ODTS-12, TC	–	8×10^{-5}	10^4	−31[a]	−32[a]

Values extracted from transfer characteristics at $V_{ds} = -60$ V, linear mobility extracted at $V_{ds} = -4$ V. BC = bottom-contact, TC = top-contact. $W/L = 500$ (this work), $W/L = 20$ [14], $W/L = 10$ [13].
V_{th} = Threshold voltage.
[a] Data estimated from published characteristics.

6. Experimental

6.1. Materials and methods

3-Tetradecylthiophene and 3-hexadecylthiophene were purchased from Carbosynth. N-Bromosuccinimide (NBS) was purchased from Acros organics. *Tert*-butyllithium, glacial acetic acid, chlorobenzene, 1,2-dichlorobenzene and Celite 545 were purchased from Merck. All other chemicals were purchased from Sigma Aldrich. All chemicals were used as received without further purification. All reactions were performed under inert (Ar) atmosphere and were monitored by thin layer chromatography (TLC, silicagel 60 F_{254} and Aluminium Oxide 150 F_{254} sheets, Merck). All column chromatography was performed with silicagel 60 (Fluka) unless stated otherwise.

All NMR spectra were measured on a Bruker Avance NMR spectrometer. ^{1}H (500 MHz) and ^{13}C (125 MHz) chemical shifts in ppm relative to TMS (0.00 ppm) or dichloromethane (5.32 ppm for ^{1}H and 54.00 for ^{13}C). q = quintet. Mass spectrometry was performed on a Thermo Fisher LTQ FT mass spectrometer in THF, a Thermo Fisher Trace DSQ II GC-MS, a Fisons GC8000-MD800 GC-MS, or a Accela LTQ FT LC-MS. IR spectroscopy was performed on a Nicolet Nexus FTIR spectrometer with a Diamond ATR cell (**1a**) or a Bruker Tensor 27 FTIR Spectrometer with a golden gate diamond ATR unit (**1b**, **1c**).

GPC traces were recorded in 80 °C ODCB on a PL-GPC120 system with a PLgel 5 μm Mixed_C column and refractive index and UV–Vis detectors. Polystyrene standards were used.

TGA measurements were performed on a Netzsch TG 209 thermo-microbalance. DSC measurements were performed on a Mettler Toledo DSC820 Calorimeter on open (hole in lid) aluminium sample pans.

UV–Vis absorption spectra were recorded on a Varian Cary 5000 double-beam UV–Vis–NIR spectrophotometer; all spectra in solution were measured from quartz cuvettes (1 cm, Hellma). Steady-state emission spectra in the spectral range of 300–800 nm were recorded on a HORIBA Jobin-Yvon IBH FL-322 Fluorolog 3 spectrometer equipped with a 450 W Xenon arc lamp, double grating excitation and emission monochromators (2.1 nm/mm dispersion; 1200 grooves/mm) and a Hamamatsu R928 photomultiplier tube or a TBX-4-X single-photon-counting detector. Emission and excitation spectra were corrected for source intensity (lamp and grating) and emission spectral response (detector and grating) by standard correction curves.

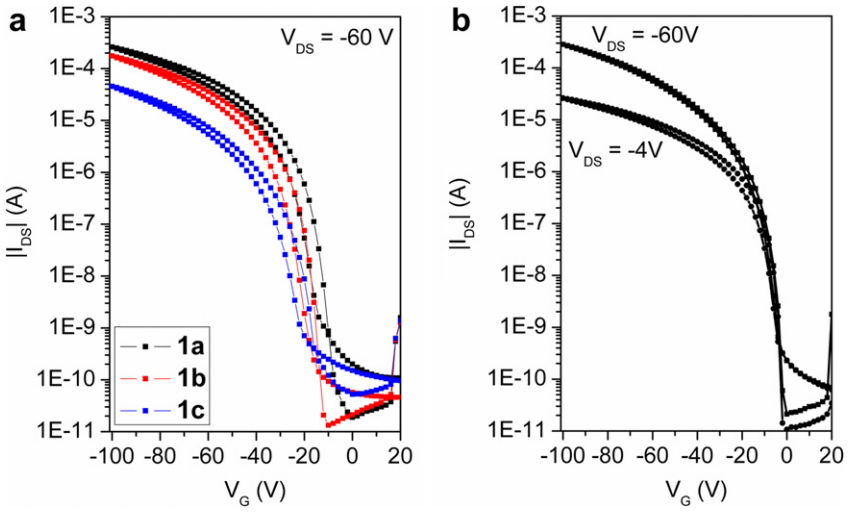

Fig. 7. Transfer characteristics of OFETs of (a) **1a**–**1c** drop cast on TMCS and (b) **1a** spun on OTS, measured in a glovebox.

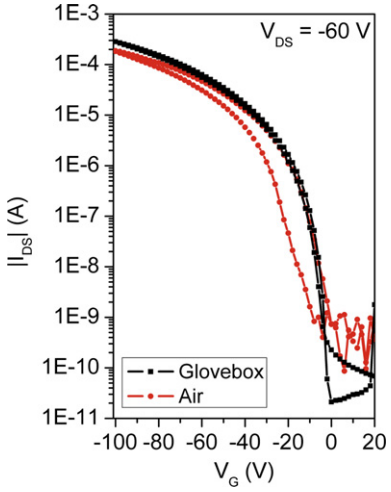

Fig. 8. Transfer characteristics of **1a**, spun on OTS in air.

Emission quantum yields were determined with a Hamamatsu Photonics absolute PL quantum yield measurement system (C9920-02) equipped with a L9799-01 CW Xenon light source (150 W), monochromator, C7473 photonic multi-channel analyzer, integrating sphere and employing U6039-05 PLQY measurement software (Hamamatsu Photonics, Ltd., Shizuoka, Japan).

A Siemens D500 Kristalloflex with a graphite-monochromized CuKα X-ray beam was used for X-ray diffraction experiments on thin films. The diffraction patterns were recorded in the 2θ range from 1° to 50° and are presented as a function of the scattering angle. The 2D-WAXS measurements were performed by means of a rotating anode (Rigaku 18 kW) X-ray beam with a pinhole collimation and a 2D Siemens detector. A double graphite monochromator for the CuKα radiation ($\lambda = 0.154$ nm) was used. The samples were prepared by filament extrusion at elevated temperatures [29].

PESA measurements were performed in air on a Riken Keiki AC2 Photoelectron spectrometer with a deuterium UV lamp and grating type monochromator. UV spot area is 4 mm^2, spectra were corrected for relative light intensity at each wavelength. PESA samples were spin-coated on OTS-pretreated SiO_2-substrates from ODCB-solutions.

OFET transfer and output characteristics were measured on an Agilent 4156C semiconductor parameter analyzer. The hole mobility μ_h (cm^2/Vs) was determined from the transfer characteristics, using the following formula [2]:

$$I_{ds} = \frac{W}{L}\mu_h C_i\left[(V_g - V_{th})V_{ds} - \frac{1}{2}V_{ds}^2\right] \quad (1)$$

where I_{ds} is the measured drain-source current (A), V_g the gate voltage (V), L the channel length (20, 10, 5 or 2.5 μm), W the channel width (0.01 m) and C_i the capacitance of the dielectric (F/cm^2). In the linear regime ($V_{ds} << V_g$), equation (1) can be rewritten, and when the derivative is taken, the linear mobility μ_{lin} can be calculated independently of V_{th} (2):

$$\mu_{lin} = \frac{\partial I_{ds}}{\partial V_g}\frac{L}{WC_iV_{ds}} \quad (2)$$

In the saturation regime ($V_{ds} \approx V_g - V_{th}$), equation (1) can be rewritten as well. Taking the square root and then the derivative, the saturation mobility μ_{sat} can be calculated independently of V_{th} (3):

$$\mu_{sat} = \left[\frac{\partial((I_{ds}))^{1/2}}{\partial V_g}\right]^2\frac{2L}{WC_i} \quad (3)$$

6.2. Monomer synthesis

Benzo[1,2-b:4,5-b′]dithiophene **2** was synthesized according to modified literature procedures [17].

^{1}H NMR (*d*-THF): δ 8.35 (s, 2H), 7.56 (d, *J* 5.5 Hz, 2H), 7.38 (d, *J* 5.5 Hz, 2H). ^{13}C NMR (*d*-THF): δ 138.7, 138.2, 128.0, 123.8, 117.5. GC-MS: found: 189.9, calculated: 189.991 g/mol ($C_{10}H_6S_2$).

6.2.1. Synthesis of 2,6-bis(tributylstannyl)benzo[1,2-b:4,5-b′] dithiophene ***3***

Glassware was dried before use. A solution of 1 g (5.26 mmol, 1 eq) **2** in 60 ml dry THF was cooled down to −80 °C. After dropwise addition of 7.5 ml *tert*-butyllithium (15% in pentane, 12.7 mmol, 2.4 eq), the mixture was allowed to slowly warm to −10 °C. The mixture was then cooled down to −50 °C again, and 3.5 ml (4.2 g, 12.7 mmol, 2.4 eq) tributylstannylchloride was added dropwise. The mixture was allowed to reach room temperature overnight.

The next morning, the mixture was quenched with 150 ml 0.1 M $NaHCO_3$, and the product was extracted with dichloromethane (4 × 60 ml). The organic phase was further washed with 0.1 M $NaHCO_3$ (2 × 60 ml), dried with Na_2SO_4, filtered and the solvent was evaporated. Column chromatography (heptane/triethylamine 95/5, neutral aluminium oxide) yielded 3.1 g of **3** as a colorless oil (76% yield).

^{1}H NMR (CD_2Cl_2): δ 8.32 (s, 2H), 7.46 (s, 2H), 1.68 (q, 12H), 1.42 (sextet, 12H), 1.25 (t, *J* 8 Hz, 12H), 0.96 (t, *J* 7.25 Hz, 18H). ^{13}C NMR (CD_2Cl_2): δ 140.6, 140.5, 137.7, 130.2, 113.8, 28.1, 26.4, 12.5, 9.9.

6.2.2. Synthesis of 2-bromo-3-tetradecylthiophene ***5b***

To a solution of 1.8 g (6.42 mmol, 1 eq) 3-tetradecylthiophene **4b** in 20 ml glacial acetic acid, 1.05 g NBS was added in small amounts over time, in absence of light. After stirring at room temperature overnight, the mixture was quenched with demineralised water (40 ml) and the product was extracted with dichloromethane (3 × 20 ml). The organic phase was washed with 1 M NaOH (2 × 30 ml), once more with brine (30 ml), dried with Na_2SO_4, filtered and the solvent was evaporated. Column chromatography (heptane) yielded 1.93 g of **5b** as a colorless liquid (84% yield).

^{1}H NMR (CD_2Cl_2): δ 7.21 (d, *J* 5.5 Hz, 1H), 6.82 (d, *J* 5.5 Hz, 1H), 2.57 (t, *J* 7.5 Hz, 2H), 1.58 (q, 2H), 1.24–1.36 (m, 22H), 0.89 (t, *J* 7 Hz, 3H). ^{13}C NMR (CD_2Cl_2): δ 142.8, 129.0, 125.8, 109.2, 32.6, 30.3 (6C), 30.2, 30.0 (3C), 29.8, 23.3, 14.5. GC-MS: found: 358.4, calculated: 358.133 g/mol ($C_{18}H_{31}SBr$).

6.2.3. 2-Bromo-3-dodecylthiophene ***5a*** *was synthesized in the same procedure as* ***5b*** *(86% yield)*

^{1}H NMR (CD_2Cl_2): δ 7.21 (d, *J* 5.5 Hz, 1H), 6.82 (d, *J* 5.5 Hz, 1H), 2.57 (t, *J* 8 Hz, 2H), 1.58 (q, 2H), 1.22–1.38 (m, 18H), 0.89 (t, *J* 7 Hz, 3H). ^{13}C NMR (CD_2Cl_2): δ 142.6, 128.7, 125.6, 108.9, 32.3, 30.1, 30.0 (3C), 29.9, 29.8, 29.7 (2C), 29.6, 23.1, 14.2. GC-MS: found: 330, calculated: 330.102 g/mol ($C_{16}H_{27}SBr$).

6.2.4. 2-Bromo-3-hexadecylthiophene ***5c*** *was synthesized in the same procedure as* ***5b*** *(87% yield)*

^{1}H NMR (CD_2Cl_2): δ 7.22 (d, *J* 6 Hz, 1H), 6.83 (d, *J* 6 Hz, 1H), 2.57 (t, *J* 8 Hz, 2H), 1.58 (q, 2H), 1.22–1.37 (m, 26H), 0.89 (t, *J* 7 Hz, 3H). ^{13}C NMR (CD_2Cl_2): δ 142.6, 128.7, 125.6, 108.9, 32.3, 30.1 (4C), 30.0 (4C), 29.9, 29.8, 29.7 (2 peaks), 29.6, 23.1, 14.2. LC-MS: found: 387.171 [M + H$^+$], calculated: 386.164 g/mol ($C_{20}H_{35}SBr$).

*6.2.5. Synthesis of 2,2′-dibromo-3,3′-bis(tetradecyl)-5,5′-bithiophene **6b** [18]*

To a solution of 0.95 g (2.64 mmol, 1 eq) **5b** in 30 ml dry DMSO, 22 mg (0.057 mmol, 0.02 eq) $PdCl_2(PhCN)_2$ and 314 mg (5.4 mmol, 2 eq) KF were added subsequently. In absence of light, 914 mg (5.4 mmol, 2 eq) $AgNO_3$ was added and the mixture was stirred at 80 °C for 4 h. After cooling down to room temperature, an additional 316 mg (5.4 mmol, 2 eq) KF and 900 mg (5.3 mmol, 2 eq) $AgNO_3$ were added and the mixture was stirred overnight at 80 °C.

The next morning, after cooling down to room temperature again, an additional 152 mg (2.62 mmol, 1 eq) KF and 450 mg (2.65 mmol, 1 eq) $AgNO_3$ were added, and the mixture was stirred at 80 °C for 4 h more. When the mixture had been cooled down to room temperature again, it was filtered over celite. The celite cake was washed thoroughly with dichloromethane. The resulting organic phase was washed with demineralised water (2 × 40 ml), the water phase was extracted with 20 ml dichloromethane. The combined organic phases were washed with demineralised water once more (40 ml), dried with Na_2SO_4, filtered and the solvent was evaporated. Column chromatography (heptane) yielded 543 mg of **6b** as a yellow solid (57% yield).

^{1}H NMR ($CDCl_3$): δ 6.76 (s, 2H), 2.51 (t, *J* 7.75 Hz, 4H), 1.57 (q, 4H), 1.23–1.37 (m, 44H), 0.88 (t, *J* 7 Hz, 6H). ^{13}C NMR ($CDCl_3$): δ 143.0, 136.2, 124.5, 107.9, 31.9, 29.7 (5C), 29.6 (3C), 29.4 (2C), 29.2, 22.7, 14.1. LC-MS: found: 715.258 [M + H^+], calculated: 714.250 g/mol ($C_{36}H_{60}S_2Br_2$).

*6.2.6. 2,2′-Dibromo-3,3′-bis(dodecyl)-5,5′-bithiophene **6a** was synthesized in the same procedure as **6b** (73% yield)*

^{1}H NMR (CD_2Cl_2): δ 6.82 (s, 2H), 2.53 (t, *J* 7.5 Hz, 4H), 1.59 (q, 4H), 1.21–1.40 (m, 36H), 0.89 (t, *J* 7 Hz, 6H). ^{13}C NMR (CD_2Cl_2): δ 143.6, 136.5, 125.0, 108.1, 32.3, 30.0 (3C), 29.9 (3C), 29.7 (2C), 29.5, 23.1, 14.2. LC-MS: found: 659.194 [M + H^+], calculated: 658.188 g/mol ($C_{32}H_{52}S_2Br_2$).

*6.2.7. 2,2′-Dibromo-3,3′-bis(hexadecyl)-5,5′-bithiophene **6c** was synthesized in the same procedure as **6b** (57% yield)*

^{1}H NMR (CD_2Cl_2): δ 6.82 (s, 2H), 2.54 (t, *J* 8 Hz, 4H), 1.59 (q, 4H), 1.21–1.40 (m, 52H), 0.89 (t, *J* 7 Hz, 6H). ^{13}C NMR (CD_2Cl_2): δ 143.6, 136.5, 125.0, 108.1, 32.3, 30.1 (5C), 30.0 (3C), 29.9 (3C), 29.7, 29.5, 23.1, 14.2. LC-MS: found: 771.319 [M + H^+], calculated: 770.313 g/mol ($C_{40}H_{68}S_2Br_2$).

6.3. General procedure for Stille copolymerization

To a dispersion of 0.25 mmol (1 eq) **3** and 0.26 mmol (1.04 eq) **6** in 6 ml dry toluene and 4 ml dry DMF, 0.005 mmol (0.02 eq) Pd$(PPh_3)_4$ was added, and the mixture was refluxed for 3 days. After cooling down to room temperature, 0.1 ml tributylphenyltin was added, and the mixture was refluxed for another 6 h. The mixture was cooled down to room temperature again to add 0.1 ml bromobenzene, and was refluxed overnight.

After cooling down to room temperature again, the mixture was poured out in methanol, and stirred for 1 h. The polymer suspension was filtered through a Soxhlet thimble, and fractionated through Soxhlet extraction (methanol, acetone, hexane, chloroform, chlorobenzene, dichlorobenzene). The chloroform, CB and ODCB fractions were taken into account to calculate the yield (relative to **3**).

*6.3.1. Poly[2,6-bis(3-dodecylthiophen-2-yl)-benzo[1,2-b:4,5-b′] dithiophene] **1a** (65% yield)*

^{1}H NMR ($CDCl_2$-$CDCl_2$): δ 8.22 (br s, 2H), 7.40 (br s, 2H), 7.07 (br s, 2H), 2.88 (br s, 4H), 1.75 (br s, 4H), 1.08–1.54 (br s + shoulder, 36H), 0.90 (br s, 6H). IR (cm^{-1}): 3060 (aromatic C–H), 2919, 2849 (–CH_2–), 1650 (C–S in BDT), 1508 (aromatic C=C), 1464 (C–S in thiophene).

*6.3.2. Poly[2,6-bis(3-tetradecylthiophen-2-yl)-benzo[1,2-b:4,5-b′] dithiophene] **1b** (50% yield)*

^{1}H NMR ($CDCl_2$-$CDCl_2$): δ 8.20 (br s, 2H), 7.37 (br s, 2H), 7.07 (br s, 2H), 2.87 (br s, 4H), 1.74 (br s, 4H), 1.05–1.57 (br s + shoulder, 44H), 0.89 (br s, 6H). IR (cm^{-1}): 3060 (aromatic C–H), 2919, 2849 (–CH_2–), 1650 (C–S in BDT), 1509 (aromatic C=C), 1464 (C–S in thiophene).

*6.3.3. Poly[2,6-bis(3-hexadecylthiophen-2-yl)-benzo[1,2-b:4,5-b′] dithiophene] **1c** (69% yield)*

^{1}H NMR ($CDCl_2$–$CDCl_2$): δ 8.21 (br s, 2H), 7.40 (br s, 2H), 7.10 (br s, 2H), 2.88 (br s, 4H), 1.74 (br s, 4H), 1.10–1.50 (br s + shoulder, 52H), 0.89 (br s, 6H). IR (cm^{-1}): 3062 (aromatic C–H), 2919, 2849 (–CH_2–), 1650 (C–S in BDT), 1510 (aromatic C=C), 1464 (C–S in thiophene).

6.4. OFET fabrication

Silicon wafers with a 230 nm thick SiO_2 dielectric and patterned gold contacts (L = 20, 10, 5, 2.5 μm, W = 0.01 m) were purchased from Fraunhofer IPMS in Dresden (D). The substrates were sonicated for 5 min in a boiling 1:1 acetone:isopropanol mixture, and afterwards washed on a spin-coater with isopropanol and demineralised water, subsequently. After heating the substrates on a hot plate at 110 °C for 1 min, the substrates were subjected to a UV/ozone treatment for 11 min.

A trimethylsilane (TMS) or octylsilane (OTS) monolayer was grown on the dielectric surface by putting the substrates in a 5% solution of trimethylchlorosilane (TMCS) in dry ethanol, respectively a 5% solution of octyltrichlorosilane (OTCS) in dry isopropanol, for 3 h. After monolayer growth, the substrates were washed with ethanol or isopropanol to remove physisorbed silane.

The polymer thin films were spin-coated (1000 rpm, 60 s) from 0.5 wt% solutions, or drop cast from 0.1 wt% solutions, of the chlorobenzene fractions of the polymers in 1,2-dichlorobenzene. The devices were annealed in a glovebox for 30 min at 130 °C before the measurements were done.

Acknowledgement

The authors thank Ralf Bovee for high-temperature GPC measurements, the European Commission for financing through the Human Potential Programme (Marie-Curie RTN NANOMATCH, Grant No. MRTN-CT-2006-035884) and the BMBF for financing through the MaDriX project.

References

[1] Allard S, Forster M, Souharce B, Thiem H, Scherf U. Angew Chem Int Ed 2008;47:4070–98.
[2] Zaumseil J, Sirringhaus H. Chem Rev 2007;107:1296–323.
[3] Leenen MAM, Arning V, Thiem H, Steiger J, Anselmann R. Phys Stat Sol (a) 2009;206:588–97.
[4] Park SK, Jackson TN, Anthony JE, Mourey DA. Appl Phys Lett 2007;91:063514.
[5] Subramanian S, Park SK, Parkin SR, Podzorov V, Jackson TN, Anthony JE. J Am Chem Soc 2008;130:2706–7.
[6] Ebata H, Izawa T, Miyazaki E, Takimiya K, Ikeda M, Kuwabara H, et al. J Am Chem Soc 2007;129:15732–3.
[7] Tsao HN, Cho D, Andreasen JW, Rouhanipour A, Breiby DW, Pisula W, et al. Adv Mater 2009;21:209–12.
[8] McCulloch I, Heeney M, Bailey C, Genevicius K, Macdonald I, Shkunov M, et al. Nat Mater 2006;5:328–33.
[9] Hamadani BH, Gundlach DJ, McCulloch I, Heeney M. Appl Phys Lett 2007;91:243512.
[10] Yan H, Chen Z, Zheng Y, Newman C, Quinn JR, Dötz F, et al. Nature 2009;457:679–86.

[11] Pan H, Li Y, Wu Y, Liu P, Ong BS, Zhu S, et al. J Am Chem Soc 2007;129:4112–3.
[12] Pan H, Wu Y, Li Y, Liu P, Ong BS, Zhu S, et al. Adv Funct Mater 2007;17:3574–9.
[13] Dang TTM, Park S-J, Park J-W, Chung D-S, Park CE, Kim Y-H, et al. J Polym Sci A 2007;45:5277–84.
[14] Rieger R, Beckmann D, Pisula W, Steffen W, Kastler M, Müllen K. Adv Mater 2010;22:83–6.
[15] Izawa T, Miyazaki E, Takimiya K. Adv Mater 2008;20:3388–92.
[16] Roichman Y, Tessler N. Appl Phys Lett 2002;80:151–3.
[17] Takimiya K, Konda Y, Ebata H, Niihara N, Otsubo T. J Org Chem 2005;70:10569–71.
[18] Takahashi M, Masui K, Sekiguchi H, Kobayashi N, Mori A, Funahashi M, et al. J Am Chem Soc 2006;128:10930–3.
[19] Masui K, Ikegami H, Mori A. J Am Chem Soc 2004;126:5074–5.
[20] Kim Y, Cook S, Kirkpatrick J, Nelson J, Durrant JR, Bradley DDC, et al. J Phys Chem C 2007;111:8137–41.
[21] Koller G, Falk B, Weller C, Giles M, McCulloch I. US 7294288 B2.
[22] Deman A-L, Tardy J, Nicolas Y, Blanchard P, Roncali J. Synth Met 2004;146:365–71.
[23] Li J, Qin F, Li CM, Bao Q, Chan-Park MB, Zhang W, et al. Chem Mater 2008;20:2057–9.
[24] De Leeuw DM, Simenon MMJ, Brown AR, Einerhand REF. Synth Met 1997;87:53–9.
[25] Umeda T, Tokito S, Kumaki D. J Appl Phys 2007;101:054517.
[26] Egginger M, Bauer S, Schwödiauer R, Neugebauer H, Sariciftci NS. Monatsh Chem 2009;140:735–50.
[27] Urien M, Wantz G, Cloutet E, Hirsch L, Tardy P, Vignau L, et al. Org Electr 2007;8:727–34.
[28] Björklund N, Lill J-O, Rajander J, Österbacka R, Tierney S, Heeney M, et al. Org Electr 2009;10:215–21.
[29] Pisula W, Tomovic Z, Simpson C, Kastler M, Pakula T, Müllen K. Chem Mater 2005;17:4296–303.